Chapter 2

Modeling Optical Scintillation

2.1 Introduction

An optical wave propagating through the atmosphere will experience irradiance (intensity) fluctuations, or *scintillation*, even over relatively short propagation paths. Scintillation is caused almost exclusively by small temperature variations in the atmosphere, resulting in index of refraction fluctuations (i.e., optical turbulence). Theoretical and experimental studies of irradiance fluctuations generally center around the *scintillation index* (normalized variance of irradiance fluctuations) defined by

$$\sigma_I^2 = \frac{\langle I^2\rangle - \langle I\rangle^2}{\langle I\rangle^2} = \frac{\langle I^2\rangle}{\langle I\rangle^2} - 1, \qquad \text{[unitless]} \tag{1}$$

where the quantity I denotes irradiance of the optical wave and the angle brackets $\langle\ \rangle$ denote an ensemble average or, equivalently, a long-time average. In weak fluctuation regimes [defined as those regimes for which the scintillation index (1) is less than unity], derived expressions for the scintillation index show that it is proportional to the *Rytov variance* for a plane wave

$$\sigma_1^2 = 1.23 C_n^2 k^{7/6} L^{11/6}, \qquad \text{[unitless]} \tag{2}$$

where C_n^2 ($m^{-2/3}$) is the index of refraction structure parameter, $k = 2\pi/\lambda$ is the optical wave number, λ (m) is wavelength, and L (m) is the propagation path length between transmitter and receiver. The Rytov variance represents the scintillation index of an unbounded plane wave in weak fluctuations based on a Kolmogorov spectrum [Eq. (6) in Chapter 1], but is otherwise considered a measure of optical turbulence strength when extended to strong fluctuation regimes by increasing either C_n^2 or the path length L, or both. It is known that the scintillation index increases with increasing values of the Rytov variance (2) until it reaches a maximum value greater than unity in the regime characterized by random focusing, so called because the focusing caused by large-scale inhomogeneities achieves its strongest effect. With increasing path length or inhomogeneity strength, the focusing effect is diminished by multiple self interference, and the peak fluctuations slowly begin to decrease, saturating at a level for which the scintillation index approaches unity from above. Qualitatively, saturation occurs because multiple self

interference causes the optical wave to become increasingly less coherent (spatially) as it propagates, eventually appearing like extended independent multiple sources, each radiating with a distinct random phase. In Fig. 2.1 we present a still photo of a typical cross section of the beam irradiance within the aperture diameter of a telescope after propagating 1000 m along a horizontal path 1–2 m above the ground.

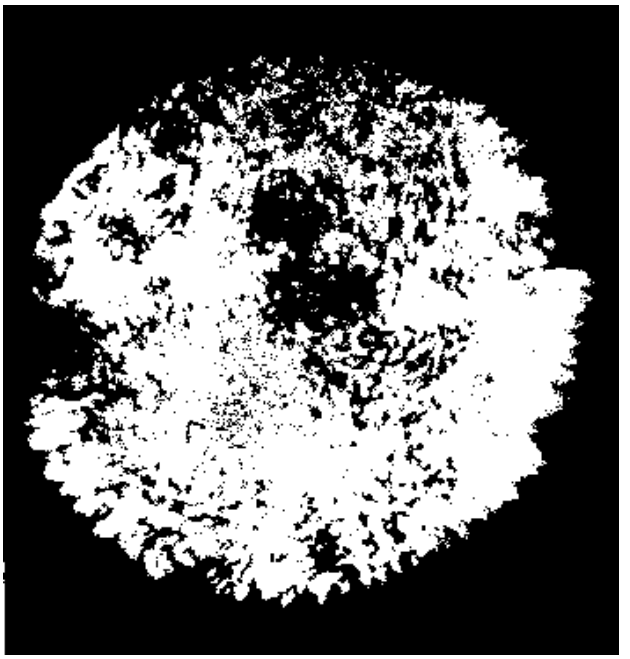

Figure 2.1 Still photo of laser beam after propagating 1000 m.

2.2 Background on Scintillation

The process of optical wave propagation through random media has been studied for many years. By random medium, we mean a turbulent medium or one for which the index of refraction of the medium exhibits random spatial variations that are large with respect to optical wavelength. As yet there is no tractable solution to the problem of irradiance fluctuations from first principles of electromagnetic wave propagation that applies to all conditions of optical turbulence. Early investigations concerning the propagation of unbounded plane waves and spherical waves through random media led to the classical monographs published in the early 1960s by Tatarskii [1] and Chernov [2], but their scintillation results were limited to weak fluctuations. The saturation effect of the optical wave was first observed

experimentally by Gracheva and Gurvich [3] in 1965. This work attracted much attention and stimulated a number of theoretical and experimental studies devoted to irradiance fluctuations under conditions of strong turbulence.

Based on weak fluctuation theory, Tatarskii [1,4] predicted that the correlation width of the irradiance fluctuations is on the order of the first Fresnel zone $\sqrt{L/k}$. The Fresnel zone defines the most effective turbulent cell size in producing scintillation at distance L from the source. That is, turbulent cell sizes smaller than the Fresnel zone contribute less to scintillation because of the weaker refractivity fluctuations associated with them, and cell sizes larger than the Fresnel zone do not diffract light through a large enough angle to reach the receiver at L. Measurements [5,6] of the irradiance covariance function under strong fluctuation conditions reveal that the correlation width decreases with increasing values of the Rytov variance σ_1^2 and that a large residual correlation tail emerges at large separation distances. In the strong fluctuation regime the correlation width of irradiance fluctuations is determined by the spatial coherence radius ρ_0 of the optical wave.

In an effort to better understand the theoretical foundation of the saturation phenomenon, several qualitative models describing the underlying physics associated with amplitude or irradiance fluctuations were developed in the mid 1970s. Yura [7] generalized Tatarskii's physical optics model to include the loss of spatial coherence of the wave as it propagates into the strong fluctuation regime. His results are primarily an order of magnitude estimate rather than a rigorous quantitative derivation, but he demonstrated that the scintillation index saturates at a value on the order of unity. Clifford et al. [8] extended Tatarskii's theory to the log-amplitude variance under strong fluctuations and showed why the smallest scales of irradiance fluctuations persist into the saturation regime. This latter model, called the heuristic theory, was subsequently modified by Hill and Clifford [9]. Although quantitative predictions from Yura's physical model and the heuristic theory of Hill and Clifford do not fully agree with other results [10,11], the basic qualitative arguments presented in these early models are still valid. The first widely accepted asymptotic theory for the saturation regime under the assumption of negligible inner scale was published in 1974 by Gochelashvili and Shishov [12]. Inner-scale models for the saturation regime were later introduced by Fante [13] for the plane wave and by Frehlich [14] for the spherical wave. Unfortunately, numerical results from all these asymptotic theories generally underpredict much of the measured data [15–18] and simulation data [19–25] for the scintillation index in the strong fluctuation regime.

2.2.1 Models for Refractive Index Fluctuations

Kolmogorov theory assumes that turbulent eddies range in size from a macroscale to a microscale, forming a continuum of decreasing eddy sizes (recall Fig. 1.3). Each eddy or cell is considered homogeneous but with a different refractive index

than its neighbors. The largest cell size smaller than those at which turbulent energy is injected into a region defines an effective outer scale of turbulence L_0, which near the ground is roughly comparable with the height of the observation point above ground. An effective inner scale of turbulence l_0, on the order of millimeters (near the ground), is identified with the smallest cell size before energy is dissipated into heat. The continuous distribution of cell sizes between the inner scale l_0 and outer scale L_0 forms the *inertial range*. Because each of the cell sizes defines a particular refractive index, the Kolmogorov theory predicts that the distribution of refractive cells between l_0 and L_0 follows an inverse power law of the physical size of the cell, with the smallest cells having the weakest refractive power and the largest cells having the strongest.

Numerical results deduced from theoretical models of scintillation depend strongly on the assumed model for the *spatial power spectrum* of refractive-index fluctuations outside the inertial range. Ignoring outer-scale effects, which are usually not included in scintillation studies, the commonly used spectral models are all specializations of (see Sec. 1.2.4)

$$\Phi_n(\kappa) = 0.033 C_n^2 \kappa^{-11/3} f(\kappa l_0), \tag{3}$$

where κ is the magnitude of the spatial wave number, l_0 is the inner scale, and $f(\kappa l_0)$ is a factor that describes inner-scale modifications of the basic power law form. The conventional *Kolmogorov power-law spectrum* is characterized by $f(\kappa l_0) = 1$, whereas $f(\kappa l_0) = \exp[-(\kappa l_0/5.92)^2]$ in the case of the *Tatarskii spectrum* [4]. Investigations [21-24,26] have shown that the *Hill spectrum* is a more accurate model for scintillation studies, but, because it is described in terms of a second-order differential equation that must be solved numerically, the Hill spectrum cannot be used in deriving analytic results. A useful analytic approximation to the Hill spectrum is given by the *modified atmospheric spectrum* [27,28] in which

$$f(\kappa l_0) = \exp\left(-\kappa^2/\kappa_l^2\right)\left[1 + 1.80(\kappa/\kappa_l) - 0.25(\kappa/\kappa_l)^{7/6}\right], \quad \kappa_l = 3.3/l_0. \tag{4}$$

Plots of the quantity $f(\kappa l_0)$ appearing in the Tatarskii spectrum and Eq. (4) for the modified atmospheric spectrum are shown in Fig. 1.9. The plot for the modified spectrum exhibits the characteristic "bump" at high wave numbers prior to the dissipation regime, but differs a little from the plot for the Hill spectrum over certain wave numbers. Nonetheless, a numerical comparison [28] of various statistical properties of the optical wave based on the modified spectrum and the Hill spectrum reveals differences that are generally within 1–2% of each other (with maximum difference of 6%). That is, integration is a smoothing process so the small difference in these particular spectrum models doesn't strongly affect numerical computation of the integrals that arise in most calculations.

In this chapter and in Chapters 3–7 we consider only the case where the refractive-index structure parameter C_n^2 is essentially constant, characteristic of a horizontal path. Modifications of the theory to accommodate slant paths will be discussed in Chapter 8.

2.2.2 Physical Model for Amplitude Fluctuations

After many years and numerous efforts, there still does not exist a rigorous theory of optical scintillation that adequately covers all fluctuation regimes. Some early attempts at modeling amplitude fluctuations through qualitative arguments did lead to the saturation effect under strong fluctuations [7,8,29], but did not address the focusing regime in which irradiance fluctuations reach peak values. Here we extend some of the early physical models to also include the focusing regime, and use these results as a basis for developing more detailed models in later chapters.

A turbulent cell or eddy in the Kolmogorov model is created by the mixing of warm and cool air. Specifically, the ground heats the air layer adjacent to it and buoyancy forces cause the warm air to rise in bubble form. The wind then shears the buoyant warm bubble of air and entrains the cooler surrounding air in a turbulent mixture. This creates a warm ambient air with cooler air entrained in swirling eddies, each of which acts on the propagating optical wave like a random focusing (or defocusing) lens. As a coherent wave begins to propagate into the atmosphere, the wave is scattered by the smallest of the turbulent cells (on the order of millimeters) through diffraction. The largest turbulent cells within the inertial range act as refractive "lenses" with focal lengths typically on the order of hundreds of meters or more. Refractive and diffractive scattering processes are compound mechanisms and the total scattering process acts like a modulation of small-scale fluctuations by large-scale fluctuations. Small-scale contributions to scintillation are associated with turbulent cells smaller than either the first Fresnel zone $\sqrt{L/k}$ or the coherence radius ρ_0, whichever is smallest. In contrast, large-scale fluctuations of the irradiance are generated by turbulent cells larger than that of either the Fresnel zone or the so-called "scattering disk" $L/k\rho_0$, whichever is largest. The scattering disk $L/k\rho_0$ is defined by the refractive cell size l at which the focusing angle $\theta_F \sim l/L$ is equal to the average diffraction angle $\theta_D \sim 1/k\rho_0$ (see Fig. 2.2).

The relative sizes of the various effective scales described above are illustrated as a function of propagation distance L in Fig. 2.3 for a propagating plane wave with wavelength $\lambda = 1.06\ \mu\text{m}$. The structure parameter is assumed to be fixed at $C_n^2 = 5 \times 10^{-13}\ \text{m}^{-2/3}$, and inner-scale and outer-scale effects are ignored. The onset of strong fluctuations occurs just beyond 200 m where the various curves intersect.

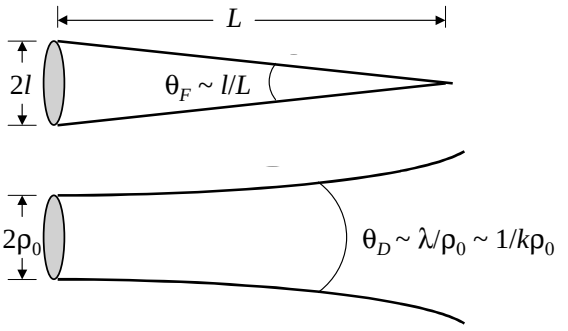

Figure 2.2 Schematic illustration of the focusing angle θ_F and diffraction angle θ_D. The scattering disk is defined as that scale size l in which these angles are equal.

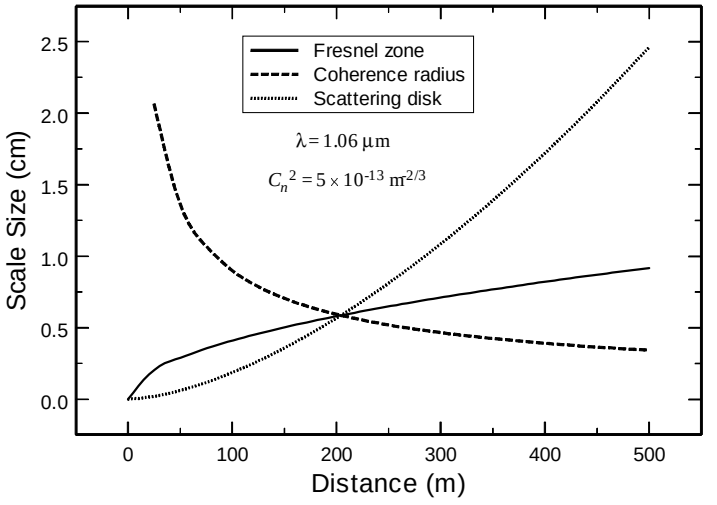

Figure 2.3 Relative scale sizes vs. propagation distance for an infinite plane wave. The point of intersection denotes the onset of strong fluctuations.

Under the assumption of statistical isotropy for the atmosphere and the paraxial approximation, a single eddy can be modeled as if it were a "thin" Gaussian-shaped dielectric lens (see Fig. 2.4). We define the radius R (m) of the Gaussian lens to be the $1/e$ distance from the center of the index distribution. Thus, if a plane wave with constant amplitude is incident on such a lens, we can use the *ABCD* ray matrix approach to infer the effective focal length of the eddy (see Sec. 1.8). The *ABCD* matrix for the eddy is given by the product

$$\begin{pmatrix} A & B \\ C & D \end{pmatrix} = \begin{pmatrix} 1 & 0 \\ \frac{n_2 - n_1}{n_2 R} & \frac{n_1}{n_2} \end{pmatrix} \begin{pmatrix} 1 & 0 \\ \frac{n_2 - n_1}{n_1 R} & \frac{n_2}{n_1} \end{pmatrix} = \begin{pmatrix} 1 & 0 \\ -\frac{\delta n}{} & 1 \end{pmatrix}, \tag{5}$$

where n_1 is the index of refraction associated with the eddy size, $n_2 \cong 1$ is the refractive index of free space, and $\delta n = n_1 - n_2 \cong n_1 - 1$. Based on Eq. (5), the effective focal distance of the eddy is

$$f \sim \frac{R/2}{\delta n}. \quad \text{[m]} \tag{6}$$

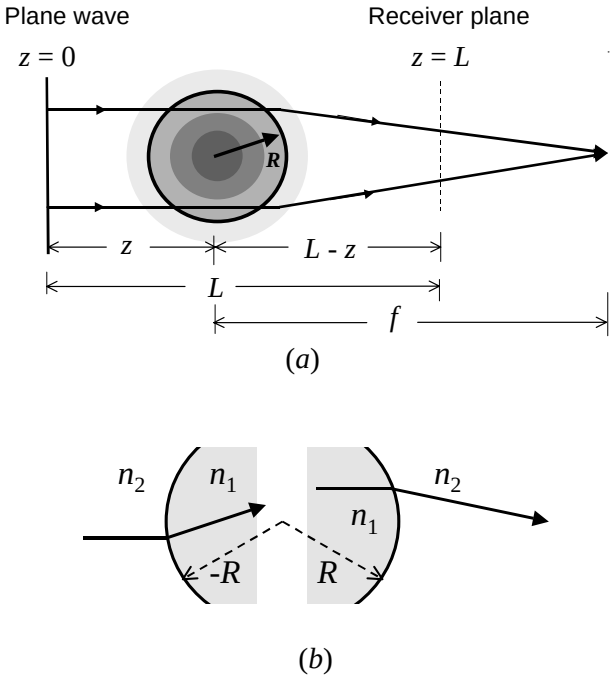

Figure 2.4 Illustration of (*a*) a plane wave incident on a single eddy modeled as a Gaussian-shaped dielectric lens with effective radius *R*, and (*b*) the interface of the left and right halves of the dielectric lens with refractive index n_1 inside the lens and n_2 outside.

If the turbulent eddy is close to the transmitter, a typical eddy size $R \sim 1$–3 cm will be larger than the Fresnel zone size but less than the coherence radius of the optical wave (e.g., see Fig. 2.3), provided the root-mean-square (rms) index of refraction difference satisfies $|\delta n| \le 10^{-6}$. In this case the plane wave incident on the eddy is considered coherent and the implied focal length from (6) is on the order of $f \sim 5$–15 km. Clearly, the average focal distance f decreases with the size R of the eddy and fixed rms refractive-index fluctuations $|\delta n|$, and also decreases with fixed eddy size and stronger rms refractive-index fluctuations $|\delta n|$.

The simplest physical model leading to optical scintillation is associated with a plane wave incident on a "sheet" of turbulent refractive cells (see Fig. 2.5) for which the sheet thickness satisfies $\Delta z \ll L - z$. For wavelengths of interest, the scattering of the optical wave by the eddies is primarily in the forward direction. Let us assume the plane wave in Fig. 2.5 is coherent in the plane $z = 0$ with constant amplitude A_0 and is propagating along the positive z-axis. In general, the wave incident on the sheet at distance $z > 0$ from the transmitter will be only partially coherent because of the loss of spatial coherence caused by atmospheric turbulence up to the sheet. By concentrating on a single eddy with radius R smaller than the coherence radius, and temporarily neglecting the effect of the random medium between the sheet and the receiver plane, we can use beam-wave analysis to express the on-axis amplitude in the receiver plane as

$$A_i = \frac{A_0}{\sqrt{(1 - z'/f)^2 + (2z'/kR^2)^2}}, \quad z' = L - z. \tag{7}$$

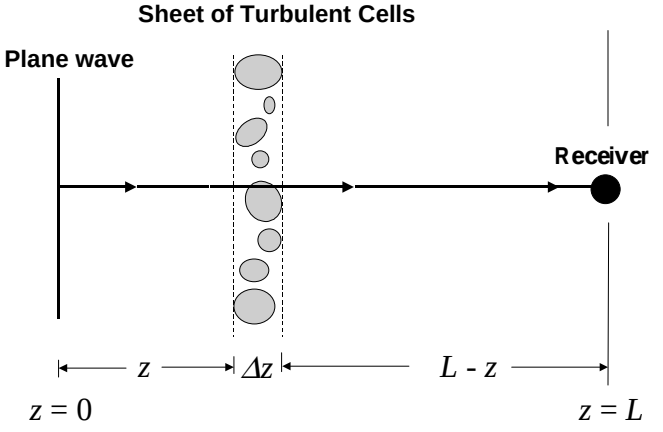

Figure 2.5 Schematic illustration of the propagation geometry for a plane wave incident on a sheet of turbulent cells (eddies).

The subscript i appearing on the left side of Eq. (7) denotes a single eddy in the sheet. Because (7) is based on an isolated finite aperture of radius R associated with the eddy, the total on-axis field amplitude in the receiver plane is given by

$$A_t = A_i + A_{\text{rest}},$$

where A_{rest} is the contribution to the field amplitude from the rest of the (empty) sheet. The quantity A_{rest} can be calculated from Babinet's principle by subtracting the portion of the wave field A_{aper} that passes through the eddy aperture from the amplitude A_0 of the incident field. This action leads to

$$A_{\text{rest}} = A_0 - A_{\text{aper}},$$

where A_{aper} can be deduced from (7) by setting $|f| = \infty$, i.e.,

$$A_{\text{aper}} = \frac{A_0}{\sqrt{1 + (2z'/kR^2)^2}}. \tag{8}$$

Hence, the total on-axis field amplitude in the receiver plane becomes

$$A_t = A_0 + A_i - A_{\text{aper}}.$$

In many practical terrestrial applications the propagation distance L from the source to the receiver will be much less than the focal distance f of the typical large eddies. Thus, by defining $\delta A_i = A_t - A_0 = A_i - A_{\text{aper}}$ and assuming $L/f \ll 1$, we obtain to a first-order approximation in L/f the amplitude fluctuations given by

$$\left\langle \left(\frac{\delta A_i}{A_0} \right)^2 \right\rangle \cong \frac{\langle (z'/f)^2 \rangle}{1 + (2z'/kR^2)^2}, \tag{9}$$

where $\langle\ \rangle$ denotes an ensemble average over the random focal lengths. By recalling the structure function relation $\langle (\delta n)^2 \rangle = C_n^2 R^{2/3}$ from Sec. 1.2.3, we can use Eq. (6) to rewrite Eq. (9) as

$$\left\langle \left(\frac{\delta A_i}{A_0} \right)^2 \right\rangle \sim \frac{C_n^2 (z')^2 R^{-4/3}}{1 + (2z'/kR^2)^2}. \tag{10}$$

We note here that the ratio $\delta A_i/A_0$ for small amplitude fluctuations is roughly the same as fluctuations in the log-amplitude (or log-irradiance) of the field [1,4].

Next, we examine the effect of the other turbulent cells in the sheet. If we sum terms like δA_i from all eddies in the sheet and assume the fields from independent eddy lenses are uncorrelated, then $\langle \delta A_i \delta A_j / A_0^2 \rangle = 0$ for $j \neq i$. Thus, the amplitude

fluctuations in the receiver plane will be essentially a sum of independent contributions from large-scale refractive eddies ($R_{\text{refract}} > \sqrt{L/k}$) and small-scale diffractive eddies ($R_{\text{diffract}} < \sqrt{L/k}$), i.e.,

$$\begin{aligned}\sigma_{\text{sheet}}^2 &\sim \sum_i \left\langle \left(\frac{\delta A_i}{A_0} \right)^2 \right\rangle_{\text{refrac}} + \sum_i \left\langle \left(\frac{\delta A_i}{A_0} \right)^2 \right\rangle_{\text{diffrac}} \\ &\sim \left. \frac{C_n^2 (z')^2 R^{-4/3}}{1 + (2z'/kR^2)^2} \right|_{R \sim R_{\text{refrac}}} \left. \frac{C_n^2 (z')^2 R^{-4/3}}{1 + (2z'/kR^2)^2} \right|_{R \sim R_{\text{diffrac}}} .\end{aligned} \tag{11}$$

To include the effect of the turbulent medium between the sheet and the receiver plane, we assume there exist many refractive and diffractive eddies of size R between the sheet and the receiver. We can then average each term in (11) over the number of these scale sizes in the propagation path, which is roughly L/R [4,29]. Also, the average of $(z')^2$ over the path is on the order of L^2. Therefore, we are led to an order of magnitude expression for the total contributions to the amplitude fluctuations given by

$$\begin{aligned}\sigma_A^2 &\sim \left. \frac{C_n^2 L^3 R^{-7/3}}{1 + (2L/kR^2)^2} \right|_{R \sim R_{\text{refrac}}} + \left. \frac{C_n^2 L^3 R^{-7/3}}{1 + (2L/kR^2)^2} \right|_{R \sim R_{\text{diffrac}}} \\ &\sim \sigma_1^2 (L/kR^2)^{7/6} \Big|_{R \sim R_{\text{refrac}}} + \sigma_1^2 (L/kR^2)^{-5/6} \Big|_{R \sim R_{\text{diffrac}}} ,\end{aligned} \tag{12}$$

where we have written $\sigma_1^2 \sim C_n^2 k^{7/6} L^{11/6}$.

Excluding the inner and outer scales, the most effective refractive and diffractive cell sizes appearing in (12) are given by

$$\begin{aligned} R_{\text{refract}} &\sim \begin{cases} \sqrt{L/k}, & \text{(weak fluctuations)} \\ L/k\rho_0, & \text{(strong fluctuations)}, \end{cases} \\ R_{\text{diffract}} &\sim \begin{cases} \sqrt{L/k}, & \text{(weak fluctuations)} \\ \rho_0, & \text{(strong fluctuations)}. \end{cases} \end{aligned} \tag{13}$$

From (12) and (13) we can deduce the general behavior of the amplitude fluctuations in various regimes by properly selecting the effective refractive and diffractive scale sizes for the given regime. For example, when the inner scale is negligible the dominant scale size under *weak fluctuations* is $R \sim \sqrt{L/k}$. In this case the refractive and diffractive terms in (12) both lead to expressions on the order of σ_1^2. However, the refractive and diffractive effects can each be only some fraction of σ_1^2

because their sum in this regime must equal σ_1^2. When inner-scale l_0 is present, it is often the dominant scale size and may be larger than the Fresnel zone (i.e., $l_0 \gg \sqrt{L/k}$). Thus, if we neglect the diffractive term in (12) and set $R \sim l_0$ in the first term, we obtain the geometrical optics result [4] $\sigma_A^2 \sim \sigma_1^2 (L/kl_0^2)^{7/6} \sim C_n^2 L^3 l_0^{-7/3}$. Although the geometrical optics approximation ignores diffraction effects, the influence of diffraction is always present and tends to weaken the focusing effect of the random large lenses.

With *strong fluctuations* approaching the *saturation regime* we consider situations in which the turbulent sheet and the receiver plane are both located farther from the source. In this case the loss of spatial coherence of the optical wave will affect which eddies in the sheet are still strong enough to focus the wave. That is, the ability of a given cell size to focus a partially coherent wave is less than that for a coherent wave. Because of the loss of spatial coherence of the optical wave under strong fluctuations, only the largest eddies near the transmitter have any effective focusing effect on the illumination of small diffractive eddies near the receiver. The loss of coherence also limits the maximum size of the effective small-scale eddies near the receiver. That is, in the saturation regime the effective small-scale eddy size is roughly that of the spatial coherence radius $\rho_0 \sim (C_n^2 k^2 L)^{-3/5}$ where $\rho_0 \ll \sqrt{L/k}$. By setting $R \sim \rho_0$ in the second expression in (12) we obtain $(\sigma_A^2)_{\text{diffrac}} \sim \sigma_1^2 (\sigma_1^2)^{-1} \sim 1$, which represents the upper bound for small-scale fluctuations. This result is the small-scale saturation effect demonstrated by Yura [7] using a more detailed analysis. Similarly, the most effective large-scale eddy size under strong fluctuations is that of the scattering disk $L/k\rho_0$. Here, the substitution of $R \sim L/k\rho_0$ into the first expression in (12) yields $(\sigma_A^2)_{\text{refrac}} \sim 1/\sigma^{4/5}$ and the sum of diffractive and refractive effects gives us $\sigma_A^2 \sim 1 + 1/\sigma^{4/5}$, $\sigma_1^2 \to \infty$. To within a scaling factor in the second term, this last result is the expression deduced from the asymptotic theory (see Sec. 1.7.2).

Between weak fluctuations and saturation lies the onset of strong fluctuations and the *focusing regime*, neither of which is a simple limiting case involving the well-defined scale sizes given in (13). Once again the large eddies near the transmitter have the greatest focusing effect on small eddies near the receiver and, consequently, are responsible for peak scintillation in the focusing regime. As the optical wave propagates beyond this regime the continued loss of spatial coherence weakens the focusing effect and eventually leads to saturation as described above. Approaching strong fluctuations the large-scale refractive cells lie somewhere between the size of the Fresnel zone and that of the scattering disk. Thus, we assume $R_{\text{refract}} \sim [L/k + (L/k\rho_0)^2]^{1/2}$, which reduces to the scattering disk under sufficiently strong fluctuations. Similarly, small-scale diffractive cells lie between the size of the Fresnel zone and the spatial coherence radius, and therefore we assume $R_{\text{difract}} \sim [1/(L/k) + 1/\rho_0^2]^{-1/2}$. In this case the sum of refractive and diffractive fluctuations deduced from Eq. (12) are of the form